# Retrograde Delivery of Photosensitizer (TPPp-O-$\beta$-GluOH)$_3$ Selectively Potentiates Its Photodynamic Activity

Mohamed Amessou,[†] Danièle Carrez,[‡,§] Delphine Patin,[†] Marianne Sarr,[†] David S. Grierson,[‡,||,⊥] Alain Croisy,[‡,§] Antonio C. Tedesco,[@] Philippe Maillard,*[,‡,||,#] and Ludger Johannes[†,#]

Institut Curie, Centre de Recherche, 26 rue d'Ulm, F-75248 Paris Cedex 05, France, CNRS UMR144, 26 rue d'Ulm, F-75248 Paris Cedex 05, France, Institut Curie, Centre de Recherche, Centre Universitaire, Université Paris-Sud, F-91405 Orsay Cedex, France, INSERM U759, Centre Universitaire, Université Paris-Sud, F-91405 Orsay Cedex, France, CNRS UMR176, Centre de Recherche, Centre Universitaire, Université Paris-Sud, F-91405 Orsay, France, and Departamento de Química, Laboratório de Fotobiologia e Fotomedicina, Faculdade de Filosofia Ciências e Letras de Ribeirão Preto, Universidade de São Paulo, Av. Bandeirantes 3900, CEP, 14040-901 Ribeirão Preto, Brazil. Received October 29, 2007; Revised Manuscript Received November 15, 2007

Photodynamic therapy involves administration of a photosensitizing drug and its subsequent activation by visible light of the appropriate wavelength. Several approaches to increasing the specificity of photosensitizers for cancerous tissues and, in particular, through their conjugation to ligands that are directed against tumor-associated antigens have been investigated. Here, we have studied the delivery of the photocytotoxic porphyrin compound TPP(p-O-$\beta$-D-GluOH)$_3$ into tumor cells that overexpress the glycosphingolipid Gb3, using the Gb3-binding nontoxic B-subunit of Shiga toxin (STxB) as a vector. To allow for site-directed chemical coupling, an STxB variant carrying a free sulfhydryl moiety at its C-terminal end has been used. Binding affinity, cellular uptake, singlet oxygen quantum yield, and phototoxicity of the conjugate have been examined. Despite some effect of coupling on both the photophysical properties of TPP(p-O-$\beta$-D-GluOH)$_3$ and the affinity of STxB for its receptor, the conjugate exhibited a higher photocytotoxic activity than the photosensitizer alone and was exquisitely selective for Gb3-expressing tumor cells. Furthermore, our data strongly suggest that STxB-mediated retrograde delivery of the photosensitizer to the biosynthetic/secretory pathway is critical for optimal cytotoxic activity. In conclusion, a strong rationale for using retrograde delivery tools such as STxB in combination with photosensitizing agents for the photodynamic therapy of tumors is presented.

## INTRODUCTION

Anticancer therapy often relies on the use of chemotherapeutic agents that efficiently eliminate dividing cancer cells. However, in many cases, chemotherapy fails to eradicate tumors, and even when chemotherapy is successful, systemic cytotoxicity often results in deleterious side effects. To overcome these limitations, novel strategies have been developed that aim at increasing the selectivity of tumor treatment. In this context, antibodies, hormones, growth factors, lectins, and toxins have been explored as tools for delivering therapeutic compounds to cancer cells (*1, 2*).

The bacterial Shiga toxins and verotoxins (or Shiga-like toxins) share a cellular receptor, the glycosphingolipid globotriaosylceramide (Gb3[1] or CD77), that is expressed on a number of human malignancies, such as Burkitt's lymphoma (*3*) and cancers of the breast (*4*), brain (*5*), ovary (*6*), colon (*7*), and testis (*8*). Shiga toxin is produced by *Shigella dysenteria*, and verotoxins are produced by enterohemorrhagic strains of *Escherichia coli* (*9*). These toxins are composed of an enzymatic component (A subunit) that inhibits protein biosynthesis by modifying rRNA and a nontoxic homopentameric component (B subunit or STxB). The A subunit cannot enter cells by itself. For plasma membrane binding and internalization, it requires a noncovalent interaction with STxB. In toxin sensitive cells, STxB delivers the holotoxin from the plasma membrane to the endoplasmic reticulum, via the early endosome and the Golgi apparatus, a transport pathway termed the retrograde route (*10, 11*). Trafficking through the retrograde route allows STxB to escape degradation in lysosomes and recycling to the plasma membrane, resulting in its stable association with cells.

Recently, the possibility of using STxB as a delivery tool for Gb3-expressing tumors has been addressed. It was shown that upon oral uptake or intravenous injection, STxB targets adenocarcinomas of the intestine in a transgenic mouse model (*12*). In the context of the holotoxin, an antineoplasic activity has been detected upon injection of verotoxin-1 into xenografted tumors (*5, 13–15*), and verotoxin-1 eliminates clonogenic tumor cells in purging applications (*16*). However, the use of holotoxin as a therapeutic agent in humans may be limited by the fact that the catalytic effect of the A subunit is not tumor specific. STxB has therefore directly been linked to therapeutic com-

* To whom correspondence should be addressed. Phone: +33 1-69 86 31 71. Fax: +33 1-69 07 53 27. E-mail: philippe.maillard@curie.u-psud.fr.

[†] Institut Curie, Centre de Recherche, and CNRS UMR144.

[‡] Institut Curie, Centre de Recherche, Centre Universitaire, Université Paris-Sud.

[§] INSERM U759, Centre Universitaire, Université Paris-Sud.

[||] CNRS UMR176, Centre de Recherche, Centre Universitaire, Université Paris-Sud.

[⊥] Present address: Faculty of Pharmaceutical Sciences, University of British Columbia, 2146 East Mall, Vancouver, BC, Canada V6T 123.

[@] Universidade de São Paulo.

[#] Principal investigators.

[1] Abbreviations: Gb3, globotiaosyl ceramide; STxB, Shiga toxin B subunit; PDT, photodynamic therapy; PPMP, 1-phenyl-2-hexadecanoyl-amino-3-morpholino-1-propanol; MTT, 3-(4,5-dimethylthiazol-2-yl)-2,5-diphenyltetrazolium bromide; TPP, tetraphenylporphyrin; LD, lethal dose; BFA, brefeldin A.

10.1021/bc7003999 CCC: $40.75 
Published on Web 01/19/2008

pounds that have selective antitumor activity (*17*) or that can be activated locally (*18*).

Photodynamic therapy (PDT) is based on the preferential accumulation of a photosensitizing molecule in malignant tissue after its systemic administration. Illumination using light of an appropriate wavelength excites the photosensitizer, and subsequent photoactivation results in the release of cytotoxic species such as singlet oxygen and free radicals which are responsible for the destruction of target tissue (*19*). Several major issues continue to limit the wider application of PDT as a cancer treatment modality, including deleterious effects related to accumulation of the photosensitizer in normal tissue as well as in tumor tissue. To overcome this problem, one strategy which is receiving considerable attention is to covalently link the photosensitizer to a carrier molecule to localize the PDT effect (for reviews, see refs *20* and *21*).

In this work, we have synthesized a new glycoporphyrin that was covalently linked to STxB. We have demonstrated that the photocytotoxic properties of the conjugate depend critically on its subcellular delivery via the retrograde route.

## MATERIALS AND METHODS

**Materials.** All solvents were reagent grade. Dry MeOH was kept over 3 Å sieves; methylene chloride was distilled from calcium hydride and kept over 4 Å sieves, and chloroform was distilled from calcium chloride and kept over 4 Å sieves. Column chromatography was performed with the indicated solvents and using E. Merck silica gel 60 (particle size of 0.035–0.070 mm). Macherey-Nagel precoated plates (SIL G-200, 2 mm) were used for preparative thin layer chromatography. Yields refer to chromatographically and spectroscopically pure compounds. $^1$H spectra were recorded on a Bruker AC-300 spectrometer at room temperature using an internal deuterium lock. Acidic impurities in $CDCl_3$ were removed by treatment with anhydrous $K_2CO_3$. Mass spectrometry analysis was performed using a MALDI-TOF mass spectrometer (PerSeptive Biosystem Voyager Elite, PerSeptive Biosystem, Framingham, MA). Quantitative UV–visible spectra were obtained using a Varian DMS 200 spectrometer. Microanalyses were performed by the ICSN-CNRS Elemental Analysis Center at Gif-sur-Yvette, France. STxB-Cys and STxB-Glyc-KDEL were prepared as previously described (*28, 36*). PD-10 gel exclusion columns (Amersham Pharmacia Biotech), 1-phenyl-2-hexadecanoylamino-3-morphorpholin-1-propanol (PPMP) (Calbiochem), secondary fluophore-coupled antibodies (Jackson Immunresearch), and 3-(4,5-dimethylthiazol-2-yl)-2,5-diphenyltetrazolium bromide (MTT) (Sigma Aldrich) were obtained from the indicated commercial sources. The protein concentration was determined by the Bio-Rad assay (Bio-Rad Laboratories). HeLa cells were cultured as published previously (*28*).

**Synthesis of TPP(p-O-β-D-GluOH)$_3$(p-CH$_2$Br).** *5,10,15-Tris[4-(2′,3′,4′,6′-tetraacetyl-O-β-D-glucosyloxyphenyl)]-20-(4-bromomethylphenyl)porphyrin (**3**).* Freshly distilled pyrrole (205 μL, 2.9 mmol) in chloroform (7.50 mL), 4-O-(2′,3′,4′,6′-tetraacetyl-β-D-glucopyranosyloxy)benzaldehyde (1 g, 2.2 mmol), and 4-bromomethylbenzaldehyde (0.147 g, 0.74 mmol) in chloroform (7.5 mL) were added to chloroform (750 mL) purged with argon for 30 min. The mixture was stirred under argon for a further 10 min. Then a $BF_3$-etherate solution in chloroform (317 μL, 0.5 M) was added, and the mixture was stirred under argon. The mixture was stirred at room temperature for 2 h. Triethylamine (305 μL) was added, and the mixture was stirred at room temperature 15 min. *o*-Chloranil (1.385 g, 5.6 mmol) was added, and the solution was stirred at room temperature for 2 h. Silica gel (10 g) was added to the dark solution, and the solvent was evaporated. The absorbed crude products were placed on the top of a chromatographic silica gel column. The porphyrin mixture was eluted with methylene chloride and acetone (10/1, v/v). The third red fraction was collected and purified again by preparative thin layer silica gel chromatography eluted with methylene chloride and acetone (10/1, v/v). The titled pure triglycosylated porphyrin **3** was obtained as red crystals after crystallization from methylene chloride and heptane (300 mg, 31% yield). Anal. $C_{87}H_{85}BrN_4O_{30}\cdot 3H_2O$. Calcd: C, 58.03; H, 5.09; N, 5.09. Found: C, 58.07; H, 4.77; N, 2.74. UV–visible spectrum in methylene chloride: $\lambda_{max}$ (nm) [$\epsilon$ (mmol$^{-1}$ cm$^{-1}$)] 419.5 (414.3), 516 (17.9), 552 (10.5), 591 (6.9), 647 (5.9). $^1$H NMR spectrum in $CDCl_3$: $\delta$ 8.88 (s, 8 H, pyrrole), 8.26 (d, 2 H, *o*-phenyl), 8.16 (d, 6 H, *o*-phenoxy), 7.82 (d, 2 H, *m*-phenyl), 7.42 (d, 6 H, *m*-phenoxy), 5.50 (m, 9 H, H "ose"), 5.33 (m, 3 H, H "ose"), 4.88 (s, 2 H, $CH_2Br$), 4.45 (dd, 3 H, $H_aC_6$ "ose"), 4.33 (d, 3 H, $H_bC_6$ "ose"), 4.08 (m, 3 H, $HC_5$ "ose"), 2.24 (s, 9 H, acetyl), 2.14 (s, 9 H, acetyl), 2.13 (s, 18 H, acetyl), −2.79 (s, 2 H, NH).

*5,10,15-Tris(4-O-β-D-glucosyloxyphenyl)-20-(4-bromomethylphenyl)porphyrin (**4**).* To a solution of **3** (50 mg, 28.6 μmol) in dry MeOH (10 mL) and dry $CH_2Cl_2$ (10 mL) was added a solution of NaOMe in MeOH (100 μL, 1 M), and the mixture was stirred for 1.5 h at room temperature. IWT TMD-8 ion-exchange resin (0.310 g) was then added, and gentle stirring was continued for 1.5 h. The reaction mixture was filtered, and the recovered resin was washed with MeOH. The combined filtrate and washings were then evaporated to dryness and crystallized from MeOH and 1,2-dichloroethane. Product **6** (33 mg, 93%) was obtained as a red powder. Anal. $C_{63}H_{61}BrN_4O_{18}\cdot 11H_2O$. Calcd: C, 52.54; H, 5.81; N, 3.89. Found: C, 52.77; H, 4.81; N, 4.08. UV–visible spectrum in DMSO: $\lambda_{max}$ (nm) [$\epsilon$ (mmol$^{-1}$ cm$^{-1}$)] 422 (373.7), 517.5 (16.2), 554 (11.5), 592.5 (6.7), 649 (6.6). $^1$H NMR spectrum in DMSO-$d_6$: $\delta$ 8.87 (s, 6 H, pyrrole), 8.82 (s, 2 H, pyrrole), 8.24 (d, 2 H, *o*-phenyl, $J = 7.9$ Hz), 8.13 (d, 6 H, *o*-phenoxy, $J = 7.9$ Hz), 7.89 (d, 2 H, *m*-phenyl, $J = 8.3$ Hz), 7.48 (d, 6 H, *m*-phenoxy, $J = 8$ Hz), 5.7 (s, 2 H, $CH_2Br$), 5.23 (d, 3 H, $HC_1$ "ose"), 3.82 (d broad, 3 H, $H_aC_6$ "ose"), 3.54 (m, 3 H, $H_bC_6$ "ose"), 3.42 (m, 3 H, $HC_3$ "ose"), −2.91 (s, 2 H, NH). $^{13}$C NMR spectrum in DMSO-$d_6$: $\delta$ 157.4 (*p*-C phenoxy), 141 (*meso*-C phenyl), 137 (*p*-C phenyl), 135.1 (*meso*-C and *m*-C phenoxy), 134.5 (*o*-C phenyl), 131 (C-H pyrrole), 127 (*m*-C phenyl), 120 (*meso*-C), 114.3 (*o*-C or *m*-C phenoxy), 100.5 ($C_1$ "ose"), 73.5 ($C_2$ "ose"), 60.7 ($C_6$ "ose"), 45.7 ($CH_2Br$). MALDI-TOF ($C_{63}H_{61}BrN_4O_{18}$): calcd 1240.32, found M + 1 1241.48.

**Chemical Coupling of STxB with TPP(p-O-β-D-GluOH)$_3$(p-CH$_2$Br).** STxB-Cys (5 mg/mL) in 20 mM borate buffer (pH 9) and 150 mM NaCl was incubated volume to volume with a 5-fold molar excess of TPP(p-O-β-D-GluOH)$_3$(p-$CH_2$Br) dissolved in DMSO. The reaction was carried out in the dark for 2 h at room temperature. The TPP(p-O-β-D-GluOH)$_3$(p-$CH_2$)−STxB conjugate was separated from monomeric TPP(p-O-β-D-GluOH)$_3$(p-$CH_2$Br) by gel filtration chromatography using PD-10 columns equilibrated with PBS and 10 mM EDTA buffer (pH 8.0).

**Mass Spectrometry Analysis.** All analyses were performed on a Voyager-DE PRO MALDI-TOF mass spectrometer (Applied Biosystems, Framingham, MA) operated in the delayed extraction and linear mode. A solution of sinapinnic acid in acetonitrile and TFA (30%/0.1%) was used as a matrix. Samples were prepared by mixing them with the matrix at a sample: matrix ratio of 1:1. The mixture (1 μL) was spotted onto a MALDI plate and allowed to dry.

**Immunofluorescence Analysis.** Immunofluorescence experiments were performed as previously described (*28*). Briefly, cells were incubated for 30 min at 4 °C with 1 μM STxB or TPP(p-O-β-D-GluOH)$_3$(p-$CH_2$)−STxB conjugate, washed, incubated for 45 min at 37 °C, fixed in 4% *p*-formaldehyde for 15 min at

room temperature, quenched with ammonium chloride, and permeabilized with 0.05% saponin. STxB was labeled with the monoclonal anti-STxB antibody (13C4) and revealed by the Cy3-coupled secondary antibody. Then coverslips were mounted and analyzed on a Leica wide field fluorescence microscope.

**Receptor Binding Assay.** STxB-Glyc-KDEL was iodinated using iodobeads as previously described (*28*). The binding affinities of the TPP(p-O-$\beta$-D-GluOH)$_3$(p-CH$_2$)−STxB conjugate and STxB-Cys for cells were compared in competition experiments. These were performed in 24-well plates ($10^5$ cells per well). Briefly, HeLa cells in triplicate were incubated for 30 min at 4 °C in complete DMEM medium with 20 nM [$^{125}$I]STxB-Glyc-KDEL (6000 cpm/ng) in the absence or presence of increasing concentrations (4 nM to 2.5 $\mu$M) of TPP(p-O-$\beta$-D-GluOH)$_3$(p-CH$_2$)−STxB conjugate or STxB-Cys. Cells were washed three times with complete DMEM medium and lysed in 2 × 0.5 mL of 0.1 M KOH buffer. Cell-associated radioactivity was determined using a gamma counter.

**Assessment of Singlet Oxygen Formation.** The singlet measurements were based on the direct determination by luminescence measurement at 1270 nm of the amount of photosensitizer-generated singlet oxygen [$\Phi_\Delta(^1O_2)$] (*37*). A frequency double Nd:YAG laser (Continuum, Santa Clara, CA) was used for excitation (8 ns half-life), and the luminescence decay kinetics were detected using a germanium detector operating at liquid nitrogen temperature. A silicon filter was used to prevent any fluorescence signal from interfering with the singlet oxygen measurement. Transient decays were averaged using a Tektronix TDS 340 digital oscilloscope and analyzed with software from Edinburgh Instruments. The experiments were conducted using pheophorbide-*a* in deuterated ethanol as a reference [$\Phi_\Delta(^1O_2) = 0.59$] (*38*). Quantum yields of singlet molecular oxygen were determined in oxygen-saturated solutions.

**Phototoxicity Assay.** HeLa cells were seeded in 96-well plates at a density of $10^5$ cells/mL (0.2 mL/well) and allowed to grow for 24 h in an incubator (5% $CO_2$, 37 °C, humidified atmosphere). On the day of the experiment, the culture medium was removed, and 200 $\mu$L of fresh DMEM medium with 2% FCS containing photosensitizers at a final concentration between 1 and 6 $\mu$M was added to each well. Cells were incubated at 37 °C for 24 h and then washed before fresh complete medium was added. Illumination was performed in sterile form for 15 min (1.8 J/cm$^2$) through the bottom of the culture plates using a "light box" made of six Philips TL 13 W tubes (total fluence of 3.8 mW/cm$^2$) covered by a diffusing glass fitted with an orange filter (0% T at 520 nm and 80% T at 590 nm), leading to a final fluence of 2 mW/cm$^2$. Controls were as follows: wells containing cells treated with the photosensitizer but not exposed to light, wells containing cells without photosensitizer and without light, and wells containing cells without photosensitizer and exposed to light. Cell viability was measured after 24 h by determination of mitochondrial activity using the MTT assay. At the time of counting, 100 $\mu$L of a DMEM/MTT (0.5 mg/mL) solution was added to each well and replaced 4 h later with 200 $\mu$L of DMSO. Optical densities of microplates were determined at 540 nm with a Bio-Rad microplate reader (model 450); survival was expressed as a percentage of untreated controls. Each experiment was carried out in triplicate.

**Brefeldin A Treatment.** Cells were incubated with the TPP(p-O-$\beta$-D-GluOH)$_3$(p-CH$_2$)−STxB conjugate (64 $\mu$g/mL) for 1 h, alone or in the presence of brefeldin A (BFA, 5 $\mu$g/mL). Cells were then washed three times at 4 °C with ice-cooled medium and illuminated as described above before reincubation at 37 °C for 24 h. Cell survival was assessed as described above and compared to unirradiated cultures as well as to BFA-treated cells without photosensitizer and untreated controls.

**Statistical Analysis.** Results are expressed as the means ± the standard error of the mean. Comparisons were made using an unpaired *t* test; a $p$ of $<0.05$ was considered to be significant.

## RESULTS

**Synthesis of Glycoconjugated Photosensitizer.** The triglucosylated porphyrin **3** (Scheme 1) is prepared by condensing pyrrole, *p*-2,3,4,6-tetraacetyl-O-$\beta$-D-glucosyloxybenzaldehyde (*22*), and bromo-*p*-tolualdehyde (*23*) (4, 3, and 1 equiv, respectively) in moderate yield (31%), using Lindsey's method (*24*). Compound **3** was purified by preparative thin layer chromatography on silica gel and characterized by physical methods. The unprotected glucoconjugated compound **4** (Scheme 1) was obtained quantitatively from **3** by treatment with MeONa and MeOH (*25*) (for experimental details, see Materials and Methods). TPP(p-O-$\beta$-D-GluOH)$_3$ (Scheme 1), the unconjugated analogue of the TPP(p-O-$\beta$-D-GluOH)$_3$(p-CH$_2$)−STxB conjugate was prepared using Oulmi's method (*26*).

**Preparation of Glycoporphyrin−STxB Conjugates.** To couple the photosensitizer **4** via its *p*-bromobenzyl substituent to a defined acceptor site on STxB, a cysteine residue was added to the C-terminal part of the protein, yielding STxB-Cys (*27*). The coupling reaction was carried out at room temperature for 2 h using a 5-fold molar excess of glycoporphyrin **4** over STxB-Cys pentamer in borate buffer containing 50% DMSO to minimize glycoporphyrin aggregation. The TPP(p-O-$\beta$-D-GluOH)$_3$(p-CH$_2$)−STxB conjugate was separated from nonconjugated compound **4** using gel filtration chromatography and analyzed using MALDI-TOF mass spectrometry. The MALDI-TOF mass spectra displayed two major peaks, one at *m*/*z* 8956 and the other at *m*/*z* 7792 corresponding to the conjugate and the nonmodified STxB-Cys, respectively (Figure 1A). Other, much less intense peaks were observed at *m*/*z* 10120, which could correspond to the coupling of two glycoporphyrin molecules to STxB, and at *m*/*z* 10389, which probably results from the reaction of the double conjugate with the sinapinnic acid matrix used for MALDI-TOF analysis.

In the next step, we examined the intracellular trafficking of the conjugate. Using immunofluorescence analysis, we could show that TPP(p-O-$\beta$-D-GluOH)$_3$(p-CH$_2$)−STxB accumulated as efficiently in the Golgi apparatus as STxB-Cys (Figure 1B), demonstrating that the functional properties of STxB were preserved.

**Characterization of the Gb3 Binding Capacity of the Conjugate.** The immunofluorescence experiment indicated that the TPP(p-O-$\beta$-D-GluOH)$_3$(p-CH$_2$)−STxB conjugate could still efficiently bind to its cellular receptor, despite the drastic coupling conditions using high DMSO concentrations and the hydrophobic nature of the glycoporphyrin. To obtain a quantitative measure of receptor binding, we performed in vitro displacement assays using an iodinated Gb3 ligand, termed [$^{125}$I]STxB-Glyc-KDEL (*28*). The iodinated ligand was incubated with cells in the presence of increasing concentrations of STxB-Cys or TPP(p-O-$\beta$-D-GluOH)$_3$(p-CH$_2$)−STxB conjugate (Figure 2). The conjugate was an efficient competitor, albeit with an IC$_{50}$ that was 5-fold higher than that of STxB-Cys. However, this slight decrease in affinity is not specific to the TPP(p-O-$\beta$-D-GluOH)$_3$(p-CH$_2$)−STxB conjugate, as it is also observed with STxB conjugates that involve antigenic proteins (not shown).

**Quantum Yield of Singlet Oxygen Formation.** Light-triggered generation of singlet oxygen by porphyrins, and other tetrapyrrole-based molecules, is the basis for the photodynamic therapy approach to eradicating cancer cells. We compared the photoefficiency of the TPP(p-O-$\beta$-D-GluOH)$_3$(p-CH$_2$)−STxB conjugate to that of analogous unconjugated TPP(p-O-$\beta$-D-GluOH)$_3$ and found that the singlet oxygen producing ability

**Scheme 1. Structure of TPP(p-O-β-D-GluOH)$_3$ and Reaction Scheme for the Synthesis of Glycoconjugated Porphyrin 4**

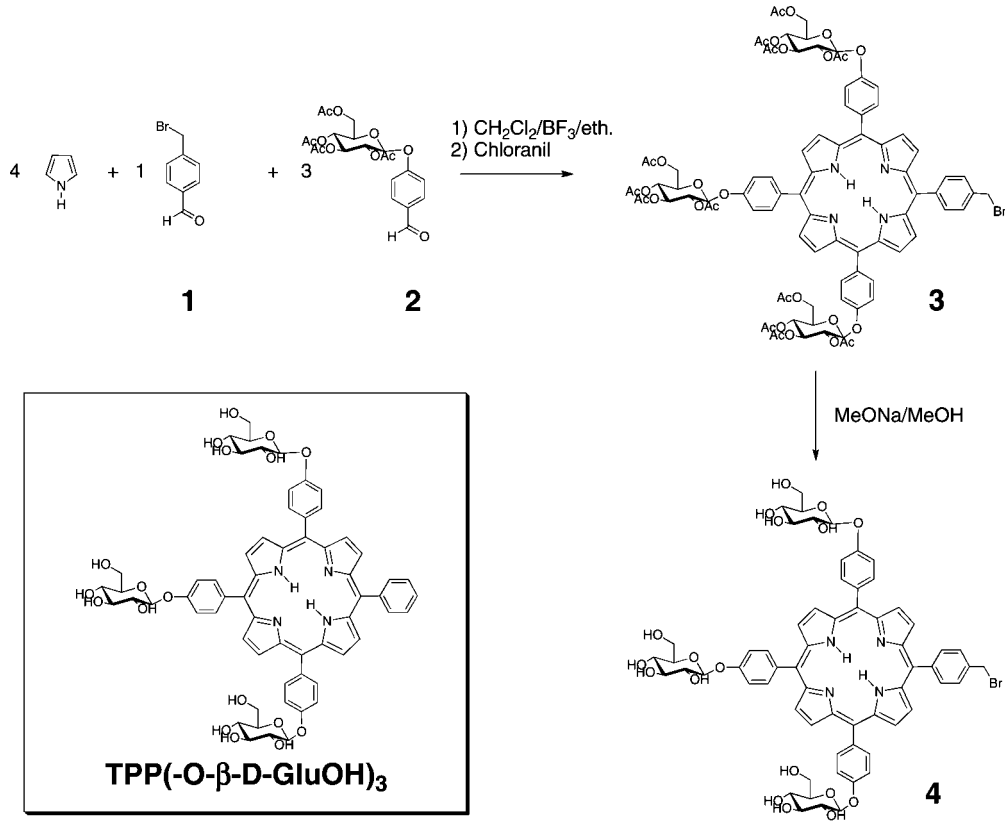


of the conjugate (0.13) was 3 times lower than that of the reference molecule (0.4). It appears that chemical coupling of **4** to STxB induces a reduction of the glycoporphyrin singlet oxygen quantum yield.

**Cellular Phototoxicity.** The phototoxicity of the free photosensitizer TPP(p-O-β-D-GluOH)$_3$ and the TPP(p-O-β-D-GluOH)$_3$(p-$CH_2$)−STxB conjugate was determined on HeLa cells after exposure to >540 nm light with a fluence of 1.8 J/cm$^2$. The presence of the STxB receptor in this cell line is well established and was confirmed using receptor binding experiments. Cells were treated with equimolar concentrations of free TPP(p-O-β-D-GluOH)$_3$ and the TPP(p-O-β-D-GluOH)$_3$(p-$CH_2$)−STxB conjugate. We observed that the conjugate was more efficient at photodynamic cell killing than TPP(p-O-β-D-GluOH)$_3$ (Figure 3). Expressed in molar concentration of photosensitizer, the $LD_{50}$ for the conjugate was 0.6 μM, and that of free TPP(p-O-β-D-GluOH)$_3$ was 3 μM, corresponding to a 5-fold sensitization. In the absence of light, toxicity was found to be negligible in all cases, with a survival fraction close to 100% (not shown). Similarly, in the absence of the TPP(p-

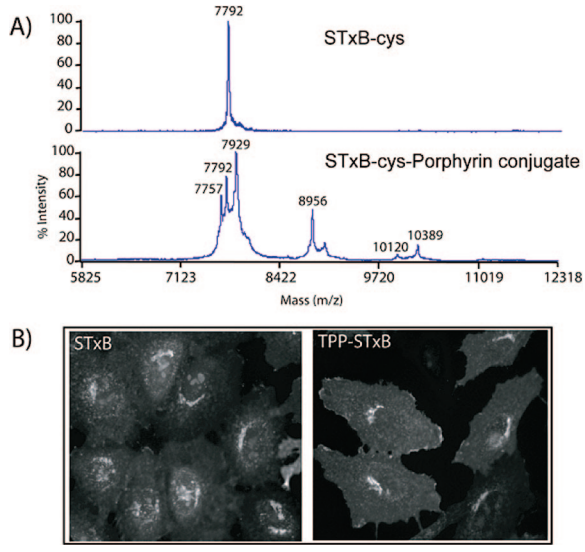


**Figure 1.** (A) MALDI-TOF mass spectra of STxB-Cys and the TPP(p-O-β-D-GluOH)$_3$(p-$CH_2$)−STxB conjugate. STxB-Cys: *m/z* 7793 (calcd) and 7792 (found). TPP(p-O-β-D-GluOH)$_3$(p-$CH_2$)−STxB conjugate: *m/z* 8954 (calcd) and 8956 (found). Note that in conjugated STxB-Cys, statistically at least one B fragment per homopentamer is modified by a TPP(p-O-β-D-GluOH)$_3$(p-$CH_2$) group. (B) Cellular uptake of STxB-Cys and the TPP(p-O-β-D-GluOH)$_3$(p-$CH_2$)−STxB conjugate. After binding at 4 °C, HeLa cells were washed and incubated at 37 °C for 45 min. The subcellular localization of STxB was determined using a mouse monoclonal anti-STxB antibody (13C4). Note that in both cases, STxB can be detected in perinuclear Golgi membranes.

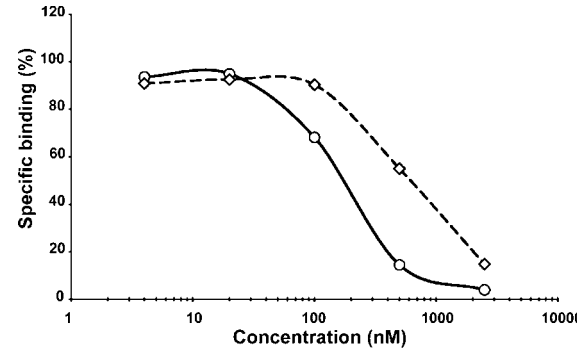


**Figure 2.** Displacement of [$^{125}$I]STxB-Glyc-KDEL from binding to Gb3-expressing cells by increasing concentrations of unlabeled STxB-Cys or TPP(p-O-β-D-GluOH)$_3$(p-$CH_2$)−STxB conjugate. HeLa cells were incubated for 30 min at 4 °C with 20 nM [$^{125}$I]STxB-Glyc-KDEL (6000 cpm/ng) either in the presence or in the absence of the indicated concentrations of unlabeled proteins. Means of two experiments carried out in triplicate: STxB-Cys (○) and TPP(p-O-β-D-GluOH)$_3$(p-$CH_2$)−STxB conjugate (◇).

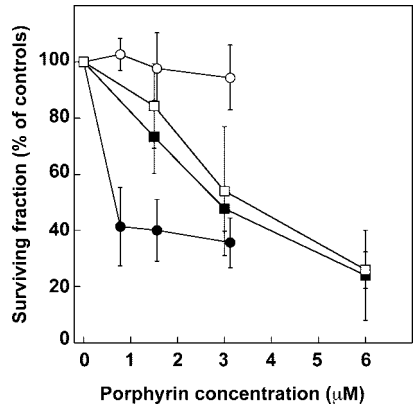


**Figure 3.** Photodynamic killing of HeLa cells with free TPP(p-O-$\beta$-D-GluOH)$_3$ or the TPP(p-O-$\beta$-D-GluOH)$_3$(p-CH$_2$)−STxB conjugate. Control or PPMP-treated HeLa cells were incubated for 24 h at 37 °C in the dark with increasing concentrations of free TPP(p-O-$\beta$-D-GluOH)$_3$ or TPP(p-O-$\beta$-D-GluOH)$_3$(p-CH$_2$)−STxB conjugate. The cells were washed three times, followed by irradiation ($\lambda$ > 540 nm) at a fluence rate of 2 mW/cm$^2$ and a light dose of 1.8 J/cm$^2$. The extent of cell death was measured by determination of mitochondrial activity using the MTT assay. The error bars represent the standard error of the mean of at least three experiments. Reported are effects of free TPP(p-O-$\beta$-D-GluOH)$_3$ in control (■) or PPMP-treated HeLa cells (□) and effects of the TPP(p-O-$\beta$-D-GluOH)$_3$(p-CH$_2$)−STxB conjugate in control (●) or PPMP-treated HeLa cells (○).

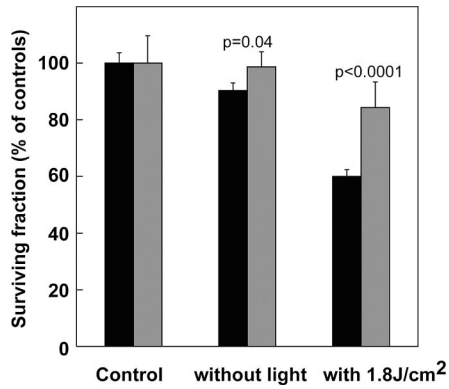


**Figure 4.** Effect of brefeldin A (BFA, 5 $\mu$g/mL) on the photocytotoxicity (1.8 J/cm$^2$) of the TPP(p-O-$\beta$-D-GluOH)$_3$(p-CH$_2$)−STxB conjugate (64 $\mu$g/mL, corresponding to 0.3 $\mu$M free porphyrin): (black bars) without BFA and (gray bars) BFA-treated.

O-$\beta$-D-GluOH)$_3$(p-CH$_2$)−STxB conjugate, cell survival was 100%, a value independent of light exposure (not shown).

To determine whether the phototoxicity of the conjugate was receptor-mediated, we performed the same experiment described above in HeLa cells in which Gb3 expression was inhibited using 1-phenyl-2-hexadecanoyl-amino-3-morphorpholin-1-propanol (PPMP) (*29*). We found that the unconjugated TPP(p-O-$\beta$-D-GluOH)$_3$ induced cell death to the same extent in Gb3-expressing and Gb3-deficient cells (Figure 3). In contrast, the conjugate induced a toxic effect in only Gb3-expressing cells, indicating that coupling to STxB provides selective means for the delivery of the photosensitizer to tumor cells (Figure 3).

**Intracellular Compartmentalization of Phototoxicity.** To measure the importance of optimal phototoxicity of retrograde delivery of TPP(p-O-$\beta$-D-GluOH)$_3$ to membranes of the biosynthetic/secretory pathway, we exploited our previous findings that treatment of cells with brefeldin A induces the accumulation of STxB in early endosomes (*30*). As shown in Figure 4, the light-induced phototoxicity of TPP(p-O-$\beta$-D-GluOH)$_3$(p-CH$_2$)-STxB was significantly higher in cells in which the conjugate was accumulated in the Golgi apparatus (column 5), when compared to cells in which the conjugate was accumulated in endosomes (column 6). In the absence of light (columns 3 and 4), the difference was much lower, and in the absence of conjugate (columns 1 and 2), it was inexistant. These data strongly suggest that the targeting of the conjugate to Golgi membranes places the photosensitizer in a molecular environment that is optimal for transducing its phototoxic effect.

## DISCUSSION

Classical cancer treatments, including surgery, radiation therapy, and chemotherapy, all cause serious side effects by the loss of normal cell function. These phenomena arise because of the lack of unambiguous, identifiable biochemical differences between normal and malignant cells. Even antibody-based approaches are confronted with severe problems that limit their use (*31*). This includes the fact that antibodies are large proteins and do not penetrate well into the tumor mass. Furthermore, antibodies remain in many cases at the cell surface or are degraded in lysosomes, thereby reducing the efficiency by which the active principle reaches intracellular sites of action. To start addressing these limitations, we have developed a PDT approach that exploits the naturally evolved capacity of STxB, a small protein, to target specific intracellular sites (*10*).

The most innovative contribution of our study consists of the demonstration that the phototoxic effect of the glycoconjugated photosensitizer directly depends on its retrograde delivery to membranes of the biosynthetic/secretory pathway. While at this stage we do not have a molecular interpretation of this finding, it is an established fact that many critical cellular functions are regulated on Golgi membranes, such as cell migration (*32*) and signaling (*33*). The localized production of short-lived singlet oxygen species and free radicals may therefore have a profound effect. Retrograde transport also provides access to the endoplasmic reticulum, which has recently been identified as a potential target for anticancer therapy (*34*). The reduced cytotoxic activity of the endosomal photosensitizer may also stem from nonoptimal pH conditions or from exposure to degrading conditions in late endosomes and/or lysosomes.

In a previous study, Tarrago-Trani et al. began exploring the use of STxB for the delivery of the photosensitizing compound chlorin e6 (*18*). However, this work was limited by the fact that no receptor-free condition was tested. In our work, we could demonstrate that the conjugated photosensitizer to Gb3-expressing cells is highly selective in that the phototoxic effect is totally lost on cells in which receptor expression has been inhibited.

As glycoporphyrins are poorly water soluble compounds, one of the principle challenges resides in making them amenable for biodistribution. Toward this end, we first exploited the fact that STxB is a very stable molecule that retains its structural integrity under extreme medium conditions and that readily recovers its native state after unfolding (*35*). Coupling and purification could therefore be conducted in 50% DMSO without significant loss of cell binding and intracellular trafficking activity. Furthermore, STxB resists extracellular inactivation and is capable of crossing tissue barriers (*12*), which should also facilitate the in vivo distribution of photosensitizers onto tumors.

The solubilization effect likely also explains why the TPP(p-O-$\beta$-D-GluOH)$_3$(p-CH$_2$)−STxB conjugate is more potent than the glycoporphyrin alone. The immunofluorescence results show that the TPP(p-O-$\beta$-D-GluOH)$_3$(p-CH$_2$)−STxB conjugate still efficiently binds to the cellular receptor Gb3. Remarkably, TPP(p-O-$\beta$-D-GluOH)$_3$ alone did not provoke any toxicity at the same dose at which the conjugate induced 50% cell death. We notice that the photosensitizing activity of the conjugated glycoporphyrin is 5 times higher than that of the parent molecule, and this despite a reduction in quantum yield after coupling.

In conclusion, our study establishes a strong rational for the use of STxB as a delivery tool for photosensitizing molecules in the development of PDT applications for the treatment of human cancers.

## ACKNOWLEDGMENT

Wolfgang Faigle, Jean-Marc Clavel, Damarys Loew (Institut Curie), and Vincent Guérineau (ICSN, CNRS) are acknowledged for their technical assistance. This work was supported by grants from Institut Curie (PIC Vectorisation), Association pour la Recherche sur le Cancer (3105 and 5177), and Fondation de France.

## LITERATURE CITED

(1) Dubowchik, G. M., and Walker, M. A. (1999) Receptor-mediated and enzyme-dependent targeting of cytotoxic anticancer drugs. *Pharmacol. Ther. 83*, 67–123.

(2) Dyba, M., Tarasova, N. I., and Michejda, C. J. (2004) Small molecule toxins targeting tumor receptors. *Curr. Pharm. Des. 10*, 2311–2334.

(3) Mangeney, M., Richard, Y., Coulaud, D., Tursz, T., and Wiels, J. (1991) CD77: An antigen of germinal center B cells entering apoptosis. *Eur. J. Immunol. 21*, 1131–1140.

(4) LaCasse, E. C., Bray, M. R., Patterson, B., Lim, W. M., Perampalam, S., Radvanyi, L. G., Keating, A., Stewart, A. K., Buckstein, R., Sandhu, J. S., Miller, N., Banerjee, D., Singh, D., Belch, A. R., Pilarski, L. M., and Gariepy, J. (1999) Shiga-like toxin-1 receptor on human breast cancer, lymphoma, and myeloma and absence from CD34(+) hematopoietic stem cells: Implications for *ex vivo* tumor purging and autologous stem cell transplantation. *Blood 94*, 2901–2910.

(5) Arab, S., Rutka, J., and Lingwood, C. (1999) Verotoxin induces apoptosis and the complete, rapid, long-term elimination of human astrocytoma xenografts in nude mice. *Oncol. Res. 11*, 33–39.

(6) Arab, S., Russel, E., Chapman, W. B., Rosen, B., and Lingwood, C. A. (1997) Expression of the verotoxin receptor glycolipid, globotriaosylceramide, in ovarian hyperplasias. *Oncol. Res. 9*, 553–563.

(7) Kovbasnjuk, O., Mourtazina, R., Baibakov, B., Wang, T., Elowsky, C., Choti, M. A., Kane, A., and Donowitz, M. (2006) The glycosphingolipid globotriaosylceramide in the metastatic transformation of colon cancer. *Proc. Natl. Acad. Sci. U.S.A. 102*, 19087–19092.

(8) Ohyama, C., Fukushi, Y., Satoh, M., Saitoh, S., Orikasa, S., Nudelman, E., Straud, M., and Hakomori, S. (1990) Changes in glycolipid expression in human testicular tumor. *Int. J. Cancer 45*, 1040–1044.

(9) O'Brien, A. D., Tesh, V. L., Donohue-Rolfe, A., Jackson, M. P., Olsnes, S., Sandvig, K., Lindberg, A. A., and Keusch, G. T. (1992) Shiga toxin: Biochemistry, genetics, mode of action, and role in pathogenesis. *Curr. Top. Microbiol. Immunol. 180*, 65–94.

(10) Johannes, L., and Decaudin, D. (2005) Protein toxins: Intracellular trafficking for targeted therapy. *Gene Ther. 16*, 1360–1368.

(11) Sandvig, K., and van Deurs, B. (2005) Delivery into cells: Lessons learned from plant and bacterial toxins. *Gene Ther. 12*, 865–872.

(12) Janssen, K.-P., Vignjevic, D., Boisgard, R., Falguières, T., Bousquet, G., Decaudin, D., Dollé, F., Louvard, D., Tavitian, B., Robine, S., and Johannes, L. (2006) *In vivo* tumor targeting using a novel intestinal pathogen-based delivery approach. *Cancer Res. 66*, 7230–7236.

(13) Ishitoya, S., Kurazono, H., Nishiyama, H., Nakamura, E., Kamoto, T., Habuchi, T., Terai, A., Ogawa, O., and Yamamoto, S. (2004) Verotoxin induces rapid elimination of human renal tumor xenografts in SCID mice. *J. Urol. 171*, 1309–1313.

(14) Heath-Engel, H. M., and Lingwood, C. A. (2003) Verotoxin sensitivity of ECV304 cells *in vitro* and *in vivo* in a xenograft tumour model: VT1 as a tumour neovascular marker. *Angiogenesis 6*, 129–141.

(15) Salhia, B., Rutka, J. T., Lingwood, C., Nutikka, A., and Van Furth, W. R. (2002) The treatment of malignant meningioma with verotoxin. *Neoplasia 4*, 304–311.

(16) LaCasse, E. C., Saleh, M. T., Patterson, B., Minden, M. D., and Gariepy, J. (1996) Shiga-like toxin purges human lymphoma from bone marrow of severe combined immunodeficient mice. *Blood 88*, 1561–1567.

(17) El Alaoui, A., Schmidt, F., Amessou, M., Florent, J. C., and Johannes, L. (2007) Shiga toxin-mediated retrograde delivery of a topoisomerase I inhibitor prodrug. *Angew. Chem., Int. Ed. 46*, 6469–6472.

(18) Tarrago-Trani, M. T., Jiang, S., Harich, K. C., and Storrie, B. (2006) Shiga-like toxin subunit B (SLTB)-enhanced delivery of chlorin e6 (Ce6) improves cell killing. *Photochem. Photobiol. 82*, 527–537.

(19) MacDonald, I. J., and Dougherty, T. J. (2001) Basic principles of photodynamic therapy. *J. Porphyrins Phthalocyanines 5*, 105–129.

(20) Wojtyk, J. T., Goyan, R., Gudgin-Dickson, E., and Pottier, R. (2006) Exploiting tumour biology to develop novel drug delivery strategies for PDT. *Med. Laser Appl. 21*, 225–238.

(21) Sharman, W. M., van Lier, J. E., and Allen, C. M. (2004) Targeted photodynamic therapy via receptor mediated delivery systems. *Adv. Drug Delivery Rev. 56*, 53–76.

(22) Halazy, S., Berges, V., Ehrhard, A., and Danzin, C. (1990) *Ortho-* and *para-*(difluoromethyl)aryl-$\beta$-image-glucosides: A new class of enzyme-activated irreversible inhibitors of $\beta$-glucosidases. *Bioorg. Chem. 18*, 330–344.

(23) Wen, L., Li, M., and Schlenoff, J. B. (1997) Polyporphyrin thin films from interfacial polymerization of mercaptoporphyrins. *J. Am. Chem. Soc. 119*, 7726–7733.

(24) Lindsey, J. S., Schreiman, I. C., Hsu, H. C., Kearney, P. C., and Marguerettaz, A. M. (1987) Rothemund and Adler-Longo reactions revisited: Synthesis of tetraphenylporphyrins under equilibrium conditions. *J. Org. Chem. 52*, 827–836.

(25) Zemplén, G. (1927) Abbau der reduzierenden biosen. *Ber. Dtsch. Chem. Ges.* 1555–1564.

(26) Oulmi, D., Maillard, P., Guerquin-Kern, J.-L., Huel, C., and Momenteau, M. (1995) Glyconjugated porphyrins. 3 Synthesis of flat amphiphilic meso-(glycosylated-aryl)-aryl porphyrins and mixed meso-(glycosylated-aryl)-alkyl porphyrins bearing some mono and disaccharide groups. *J. Org. Chem. 60*, 1554–1564.

(27) Haicheur, N., Benchetrit, F., Amessou, M., Leclerc, C., Falguières, T., Fayolle, C., Bismuth, E., Fridman, W. H., Johannes, L., and Tartour, E. (2003) The B-subunit of Shiga toxin coupled to full-size protein elicits humoral and cellular immune responses associated with a TH1 dominant polarization. *Int. Immunol. 15*, 1161–1171.

(28) Johannes, L., Tenza, D., Antony, C., and Goud, B. (1997) Retrograde transport of KDEL-bearing B-fragment of Shiga toxin. *J. Biol. Chem. 272*, 19554–19561.

(29) Abe, A., Inokuchi, J., Jimbo, M., Shimeno, H., Nagamatsu, A., Shayman, J. A., Shukla, G. S., and Radin, N. S. (1992) Improved inhibitors of glucosylceramide synthase. *J. Biochem. 111*, 191–196.

(30) Mallard, F., Tenza, D., Antony, C., Salamero, J., Goud, B., and Johannes, L. (1998) Direct pathway from early/recycling endosomes to the Golgi apparatus revealed through the study of Shiga toxin B-fragment transport. *J. Cell Biol. 143*, 973–990.

(31) Sharkey, R. M., and Goldenberg, D. M. (2006) Targeted therapy of cancer: New prospects for antibodies and immunoconjugates. *CA Cancer J. Clin. 56*, 226–243.

(32) Mellor, H. (2004) Cell motility: Golgi signalling shapes up to ship out. *Curr. Biol. 14*, R434–R435.

(33) Mor, A., and Philips, M. R. (2006) Compartmentalized Ras/MAPK signaling. *Annu. Rev. Immunol. 24*, 771–800.

(34) Boelens, J., Lust, S., Offner, F., Bracke, M. E., and Vanhoecke, B. W. (2007) Review. The endoplasmic reticulum: A target for new anticancer drugs. *In Vivo 21*, 215–226.

(35) Pina, D. G., Gomez, J., Villar, E., Johannes, L., and Shnyrov, V. L. (2003) Thermodynamic analysis of the structural stability of Shiga toxin B-subunit. *Biochemistry 42*, 9498–9506.

(36) Mallard, F., and Johannes, L. (2003) Shiga toxin B-subunit as a tool to study retrograde transport. In *Methods in Molecular Medicine: Shiga Toxin Methods and Protocols* (Philpott, D., and Ebel, F., Eds.), Vol. 73, Chapter 17, pp 209–220.

(37) Bautista-Sanches, A., Kasselouri, T., Desroches, M. C., Blais, J., Maillard, P., de Oliveira, D. M., Tedesco, A. C., Prognon, P., and Delaire, J. (2005) Photophysical properties of glucoconjugated chlorins and porphyrins and their associations with cyclodextrins. *J. Photochem. Photobiol., B 81*, 154–162.

(38) Spiller, W., Kliesch, H., Wohrle, D., Hackbarth, S., Roder, B., and Schnurpfeil, G. (1998) Singlet oxygen quantum yields of different photosensitizers in polar solvents and micellar solutions. *J. Porphyrins Phthalocyanines 2*, 145–158.

BC7003999